# Design and Fabrication of a C-Shaped Oscillating Heat Pipe with Integrated Heat Sink via Laser Powder Bed Fusion

Ishfaqur Rahman[1], Scott Thompson[2*]

[1]Department of Mechanical and Aerospace Engineering, University of Missouri, Columbia, MO 65211, United States of America.

[2]Department of Mechanical and Aerospace Engineering and University of Missouri Research Reactor (MURR), University of Missouri, Columbia, MO 65211, United States of America.

*Corresponding author: smthompson@missouri.edu

## Abstract

The design and fabrication of a “C-shaped” oscillating heat pipe (OHP) using laser powder bed fusion (L-PBF) were experimentally investigated. The structure integrates multiple conventional OHP designs into a continuous loop, forming a compact and geometrically complex thermal pathway. An integrated de-powder management strategy was incorporated into the design to enable effective powder removal from internal channels. A water block was also integrated above the OHP structure to function as a heat sink for enhanced thermal management. A prototype was fabricated to evaluate internal channel formation, de-powdering effectiveness, and overall structural fidelity through visual inspection and basic operational verification. Results demonstrate that L-PBF can successfully produce intricate OHP structures with embedded thermal management components. While dimensional and performance optimization are ongoing, the fabricated prototype confirms the feasibility of manufacturing complex passive cooling devices with integrated de-powdering and heat sinking features using L-PBF.

**Keywords:** laser powder bed fusion, oscillating heat pipe (OHP), additive manufacturing, heat exchanger design, de-powdering strategy, water block heat sink

## 1. Introduction

Oscillating heat pipes (OHPs) are passive, two-phase thermal transport devices that use a continuous serpentine network of capillary-scale channels partially filled with a working fluid. When heat is applied at one section and removed at another, vapor generation and condensation create alternating slugs of liquid and vapor whose pressure pulses drive self-sustained oscillatory flow. This cyclic motion enhances convective and latent heat transfer throughout the channel network, promoting rapid heat redistribution with minimal temperature gradients [1]. OHP behavior typically exhibits a startup threshold in heat input, followed by quasi-periodic temperature and pressure fluctuations that indicate active oscillation. Performance depends on parameters such as hydraulic diameter relative to the fluid’s capillary length, fill ratio, working-fluid properties, and the overall channel geometry and orientation [2].

Additive manufacturing (AM) expands the design space for thermal devices by enabling embedded channels, integrated manifolds, and geometries impractical with conventional fabrication. Among metal AM processes, laser powder bed fusion (L-PBF) is widely adopted for such components, offering fine feature resolution, dimensional accuracy, and the ability to realize intricate internal passages within a single build. Modern OHPs increasingly require nontraditional footprints, channel scales, and loop topologies [3]; L-PBF is well suited to meet these needs and to co-fabricate features such as charging ports and cold plates [4]. Prior demonstrations of printed OHPs have established practical strategies for powder removal and post-processing, provided guidance on channel sizing for capillary-scale operation, and validated two-phase oscillatory performance in additively manufactured structures [5], [6], [7], [8], [9].

In this work, a compact "C-shaped" OHP with an integrated water block is designed and fabricated by L-PBF and experimentally evaluated under controlled heating and cooling conditions. The study characterizes the thermal behavior of the device using distributed surface thermocouples and demonstrates the potential of this architecture for efficient, monolithic thermal management.

## 2. C-Shaped OHP Design & Manufacturing

A C-shaped OHP was designed for effective L-PBF and post-AM machining/joining operations. As shown in Fig. 1(a), the lower leg of the C-shaped structure serves as the evaporator and the upper leg of the C-structure as the condenser, and vertical passages connect the two legs to complete multiple turns. The overall footprint is 80 × 30 × 21 mm. Each channel has a 1 × 1.5 $mm^2$ rectangular cross section, a hydraulic diameter of 1.5 mm, and a length of 67.5 mm per pass with a 3 mm center-to-center pitch. The OHP consists of eight planar turns in the evaporator and condenser. An integrated charging port with approximately 6 mm outer radius and approximately 3 mm thickness is connected to both the top and bottom channel manifolds. On the side opposite the charging port, eight de-powdering holes connect to the top and bottom channels, four at the top and four at the bottom. The internal flow passage volume, computed using CAD software, was found to be approximately 10 $cm^3$. Above the C-shaped OHP is an integrated water block (cold plate), fabricated as part of the main body, providing a cooling surface area of 5 × 26 $mm^2$. The heat exchange surface (along the floor of the waterblock) comprises cylindrical pin fins of radius 1 mm, approximately 280 in count, with a fin height of 1 mm. The inlet and outlet are formed by 1 mm thick cylindrical posts that also function as de-powdering aids.

Parts were fabricated (i.e., printed) from SS316L powder using a TRUMPF TruPrint 2000 L-PBF. The powder was MetcoAdd™ 316L-A (Oerlikon), gas atomized, 15 to 45 µm particle size distribution, with apparent and tap density greater than 4 g $cm^{-3}$. The TruPrint 2000 employs dual lasers rated up to 300 W each. The major process parameters include: layer thickness of 20 µm, laser power of 113 W, hatch spacing of 0.08 mm, scan speed of 1000 mm $s^{-1}$, substrate preheat temperature of 200 °C, volumetric energy density of 70.6 J $mm^{-3}$, and nitrogen shielding gas.

Figure 1(b) shows the printed part on the build plate with support structures. The part was printed in an orientation and with an external support strategy selected to prevent internal channel collapse and heat entrapment. After fabrication, the part was removed from the baseplate using a bench saw and polished to remove excess surface material. The charging port and the eight de-powdering holes provided access for powder removal from the internal passages.

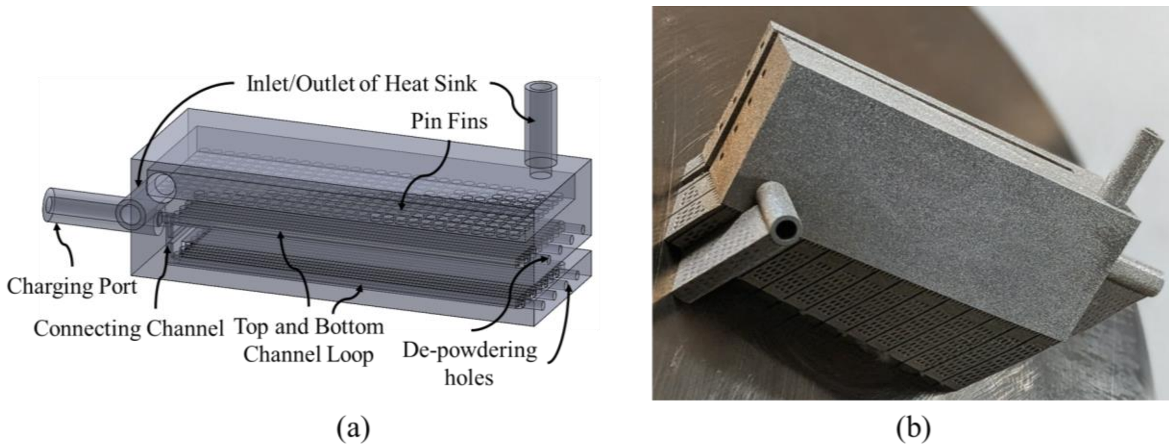


Figure 1: C-shaped OHP with integrated cold plate: (a) CAD model showing charging port, connecting channels, inlet and outlet ports, and pin-fin array; (b) additively manufactured SS316L part on the build plate with support structures.

## 3. Experimental Procedure and Setup

The experimental evaluation of the C-shaped OHP was carried out using a custom-built test assembly to assess thermal performance under controlled conditions. After printing, entrapped powder inside the OHP was removed through sequential processes of applied air pressure and fluid flushing, and the part was weighed using a precision digital scale to ensure complete removal. The de-powdering holes were then welded shut to ensure a hermetic seal. The OHP was evacuated using a laboratory-grade vacuum pump (RZ 6, VACUUBRAND) connected via a rubber-sealed charging port. The vacuum line assembly comprised a valve, rigid piping, and rubber tubing connected directly to the OHP charging port. A vacuum pressure of approximately $8.74 \times 10^{-2}$ torr was achieved, confirming a hermetically sealed environment free from leaks. The established vacuum pressure within the OHP was then used to pull room-temperature deionized (DI) water from a gas-tight syringe. The water inside the syringe was verified to not have a visible gas bubble (to maintain charging integrity). Approximately 4 mL of DI water, corresponding to ~40% of the internal volume of the OHP, was successfully charged. After charging, the valve was closed, and the rubber tubing was manually crimped to isolate the charging port from the vacuum pump. The device was subsequently weighed to obtain an initial reference mass, and was then emptied through the charging port, allowing the vacuum within the channel to draw in the water without applied force. After water injection, the rubber tubing was re-crimped securely, and the system was re-weighed to confirm accurate charging without air entrapment.

For characterizing the heat transfer performance of the OHP an experimental apparatus with controllable heat input and cooling was employed. Heating was supplied by two cartridge heaters rated at 100 W each. The heaters were inserted into a machined aluminum block that served as the evaporator interface and was mechanically secured to the bottom leg of the OHP using a C-clamp, as shown in Fig. 2. Power to the cartridge heaters was varied and controlled by a bench-top variable voltage transformer (Variac, 120 V input, 50/60 Hz, 1400 VA), and actual input was monitored with a digital multimeter (DMM). The OHP and heater block were wrapped with fiberglass insulation and suspended in a test frame to minimize environmental heat loss. Based on calibration, the heat loss from the insulated assembly was estimated to be between 5 and 6%

depending on power input. The condenser section of the OHP was connected to a closed-loop water chiller system maintained at 15 °C (± 0.2 ºC) and a constant flow rate during all tests. Seven thermocouples were bonded to the OHP surface with Loctite® 495 adhesive: two (TC 2 and TC 3) on the lower leg of the C-shaped OHP, positioned directly above the heater; three (TC 4, TC 5, and TC 6) on the side walls, with two adjacent to the lower leg and one on the upper leg; one (TC 7) near the connecting channel close to the charging port; and one (TC 1) on the inner bottom surface of the upper leg, located between the two C-shaped legs, as shown in Fig. 2. Five Type J and two Type K thermocouples were employed. Temperature data were collected at 1 Hz using an Omega TC-08 data acquisition module and logged onto a personal computer with Omega software. The software was configured to recognize thermocouple type, allowing simultaneous acquisition from both J- and K-Type thermocouples.

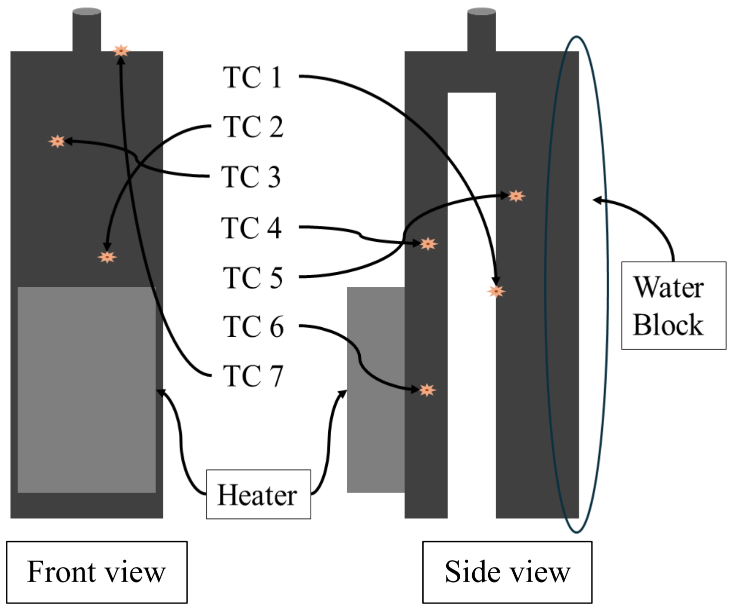


Figure 2: Front and side views of the C-shaped OHP, showing heater placement, water block, and thermocouple (TC) locations.

## 4. Results & Discussion

The C-shaped OHP tested while in a vertical orientation, with the evaporator located at the bottom surface of the lower leg of the C-shaped OHP and the condenser located adjacent to the water block on the upper leg, as shown in Fig. 2. Figure 3 presents the representative temperature response for a power input of ~58 W over a five-minute window after thermal stabilization.

The measured temperature field revealed active oscillatory behavior in the evaporator leg, consistent with the onset of slug/plug oscillations within the working fluid of an operating OHP. In particular, TC3, bonded to the bottom wall directly above the heater, exhibited repeated fluctuations in the range of 49-56 °C. These oscillations correspond to cyclic rewetting of the heated surface by liquid slugs and subsequent vapor generation, confirming that the OHP entered the expected two-phase operating regime at this heat load. TC2, located just above the heater, maintained a higher baseline temperature near 103-106 °C, while TC6, mounted on the adjacent side wall, tracked closely at ~100-102 °C. The small temperature difference between TC2 and TC6 (typically 3-5 °C) indicates that lateral conduction and liquid return effectively limited thermal buildup in the evaporator leg.

On the condenser side, TC5 remained near 64-66 °C with only gradual variation, while TC1, positioned at the top inner surface between the two legs, was stable around 45-46 °C. These measurements confirm efficient heat spreading across the top leg and consistent thermal contact with the integrated water block. TC7, located near the charging port and connecting channel, remained close to ambient (~22-23 °C) throughout the test, further verifying that heating was localized within the active evaporator-condenser pathway rather than extending into ancillary structures.

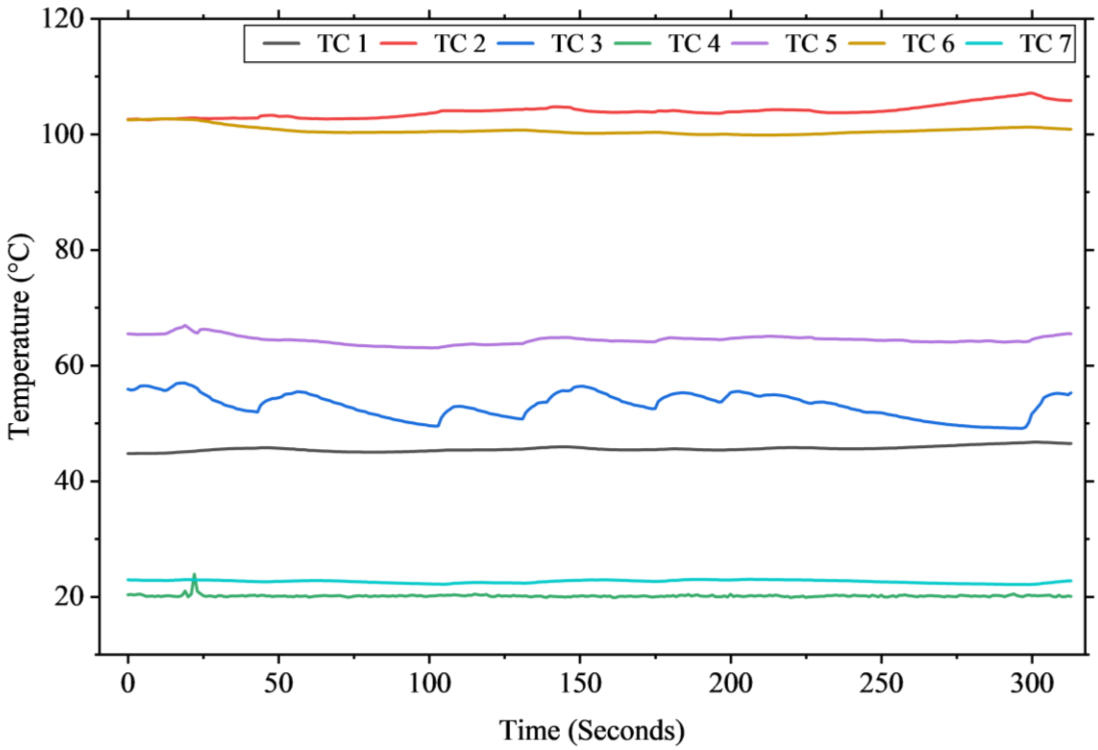


Figure 3: Steady-state temperature response of the C-shaped OHP under vertical orientation with a power input of ~58 W for ~300 seconds.

A noteworthy feature is the interplay between TC2, TC3, and TC6. The bottom wall (TC3) displayed stronger oscillations than either the heater-adjacent point (TC2) or the side wall (TC6). This behavior suggests that phase-change dynamics were concentrated within the lower channels directly exposed to the applied heating, while the surrounding metal structure maintained a relatively steady temperature field. The limited thermal gradient between evaporator and condenser thermocouples further indicates that the device was transporting heat effectively, with a net thermal drop across the structure on the order of only 40-50 °C despite the ~58 W applied load. As the OHP body was fabricated from SS316L, which has a comparatively low bulk thermal conductivity (~16 W/m·K), the overall performance may have been restricted by conduction losses in the metal structure. This highlights the potential benefit of alternative alloys or hybrid material strategies for future designs.

## 5. Conclusions

The compact L-PBF-fabricated C-shaped OHP with an integrated water block demonstrated sustained two-phase oscillation under ~58 W heat input using DI water as the working fluid and 15 °C water as coolant in the water block. Temperatures near the heater remained highest, while the condenser side stayed comparatively lower and stable, confirming effective thermal coupling to the integrated cold plate. These findings validate the feasibility of the C-shaped architecture with embedded cooling and establish a basis for future studies under varied operating conditions.

**Acknowledgments**

The authors gratefully acknowledge the University of Missouri (MU) Materials Science & Engineering Institute (MUMSEI) for supporting this study. The authors also thank Mr. James West, MU College of Engineering, for his assistance with post-processing of the printed OHP.

**References**

[1] S. M. Thompson, H. Lu, and H. Ma, "Thermal spreading with flat-plate oscillating heat pipes," in *Journal of Thermophysics and Heat Transfer*, American Institute of Aeronautics and Astronautics Inc., 2015, pp. 338–345. doi: 10.2514/1.T4168.

[2] H. B. Ma, B. Borgmeyer, P. Cheng, and Y. Zhang, "Heat Transport Capability in an Oscillating Heat Pipe," *J Heat Transfer*, vol. 130, no. 8, May 2008, doi: 10.1115/1.2909081.

[3] C. Czajkowski, A. I. Nowak, and S. Pietrowicz, "Flower Shape Oscillating Heat Pipe – A novel type of oscillating heat pipe in a rotary system of coordinates – An experimental investigation," *Appl Therm Eng*, vol. 179, p. 115702, 2020, doi: https://doi.org/10.1016/j.applthermaleng.2020.115702.

[4] O. T. Ibrahim *et al.*, "An investigation of a multi-layered oscillating heat pipe additively manufactured from Ti-6Al-4V powder," *Int J Heat Mass Transf*, vol. 108, pp. 1036–1047, 2017, doi: https://doi.org/10.1016/j.ijheatmasstransfer.2016.12.063.

[5] S. M. Thompson, Z. S. Aspin, N. Shamsaei, A. Elwany, and L. Bian, "Additive manufacturing of heat exchangers: A case study on a multi-layered Ti–6Al–4V oscillating heat pipe," *Addit Manuf*, vol. 8, pp. 163–174, 2015, doi: https://doi.org/10.1016/j.addma.2015.09.003.

[6] C. Chang, Y. Yang, L. Pei, Z. Han, X. Xiao, and Y. Ji, "Heat Transfer Performance of 3D-Printed Aluminium Flat-Plate Oscillating Heat Pipes for the Thermal Management of LEDs," *Micromachines (Basel)*, vol. 13, no. 11, Nov. 2022, doi: 10.3390/mi13111949.

[7] X. Xiao, Y. He, Q. Wang, Y. Yang, C. Chang, and Y. Ji, "Heat Transfer Performance of a 3D-Printed Aluminum Flat-Plate Oscillating Heat Pipe Finned Radiator," *Nanomaterials*, vol. 14, no. 1, Jan. 2024, doi: 10.3390/nano14010060.

[8] K. L. Chen, K. Y. Luo, P. P. Gupta, and S. W. Kang, "SLM Additive Manufacturing of Oscillating Heat Pipe," *Sustainability (Switzerland)*, vol. 15, no. 9, May 2023, doi: 10.3390/su15097538.

[9] F. Belfi, F. Iorizzo, C. Galbiati, and F. Lepore, "Space Structures With Embedded Flat Plate Pulsating Heat Pipe Built by Additive Manufacturing Technology: Development, Test and Performance Analysis," *J Heat Transfer*, vol. 141, no. 9, Jul. 2019, doi: 10.1115/1.4042082.